# A Method and a GUI for the Creation of Azimuth-Track Level-Pointing-Error Corrections

*E. Maneri*[1] *and W. Gawronski*[2]

[1]Massachusetts Institute of Technology, Cambridge, MA, USA
E-mail: emaneri@mit.edu

[2]Jet Propulsion Laboratory, California Institute of Technology
Communications Ground Systems Section, MS 238-528, Pasadena, CA 91109, USA
Tel: +1 (818) 354-1783; Fax: +1 (818) 393-0207; E-mail: wodek.k.Gawronski@jpl.nasa.gov

## Abstract

The JPL beam-waveguide (BWG) antennas are used for spacecraft tracking and for radio-astronomy observations. They are mounted on wheels that rotate around an uneven azimuth track, causing antenna deformations, and reducing pointing accuracy. The pointing errors affected by the track irregularities are repeatable, and can therefore be calibrated. The effects of the irregularities of the track can continually be corrected by using a lookup table, created by the interface presented below.

This paper is a continuation of previous work [1] appearing in this *Magazine*. It describes the processing the inclinometer data, which includes the verification of repeatability, smoothing, slow-trend removal, re-sampling, and adjustment to a standard format. It also presents a user-friendly interface that process field data and creates a lookup table for pointing-error correction by clicking appropriate buttons on a computer screen. The GUI was tested with the JPL BWG antennas, and may be used with any antennas utilizing an azimuth track.

Keywords: Space vehicle tracking; scanning antennas; pointing systems; antenna mechanical factors; antenna tolerance analysis; satellite tracking; satellite communications

## 1. Introduction

The JPL beam-waveguide (BWG) antennas are used for tracking spacecraft and for radio-astronomy observations. The alidade of the BWG antennas is mounted on wheels that move on a circular track, allowing rotation about the azimuth axis. The azimuth track is not perfectly flat. Its profile, measured at the DSS26 antenna, is shown in Figure 1, with a maximum profile deviation of 1.2 mm. An uneven azimuth track causes antenna tilts and flexible deformations, which reduce the antenna pointing accuracy during tracking.

Inclinometers have been placed high on the alidade structure, to measure structural twisting and bending due to track irregularity. Their locations are shown in Figure 2, along with the $(x, y, z)$ coordinate system. The $x$ axis is the antenna-elevation axis, directed from Inclinometer 2 to Inclinometer 1. The $z$ axis is a vertical axis, oriented downward. The $y$ axis is a horizontal axis, orthogonal to the $x$ and $z$ axes, oriented to define a right-handed coordinate system. Measuring tilts of the alidade structure at the predetermined points and processing the data provide alidade rotations in the $x$, $y$, and $z$ directions as a function of azimuth position (this function is called the lookup table), and, consequently, the pointing errors as a function of the antenna-azimuth position.

The measurements, data processing, and lookup table creation were described in [1]. The present paper expands upon the previous data-processing requirements to obtain a lookup table of greater repeatability and accuracy. It also describes the interface that makes the creation of the lookup table user friendly, with a simple format. The software and GUI (graphical user interface) presented here are generic, and not specific to a single antenna. Given data from four inclinometers, their relative positions, and azimuth-encoder data, the GUI can be used for an arbitrary antenna that uses an azimuth track.

## 2. Data Collection

The data are collected while the antenna rotates in azimuth, with inclinometers at four antenna locations, as shown in Figure 2. Each inclinometer measures $x$ and $y$ tilts. To create a lookup table, the $x$ tilts of all four inclinometers and the $y$ tilt of Inclinometer 2 are combined as described below. The antenna rotates from one extreme azimuth position (usually, $-10°$) to another (usually, $359°$) to cover at least $365°$ of rotation. The data are collected while moving clockwise and counter-clockwise, at a frequency of 2 Hz, while the antenna rotates at 50 mdeg/s. The inclinometer data are sampled every $0.025°$ of motion. At least two sets of

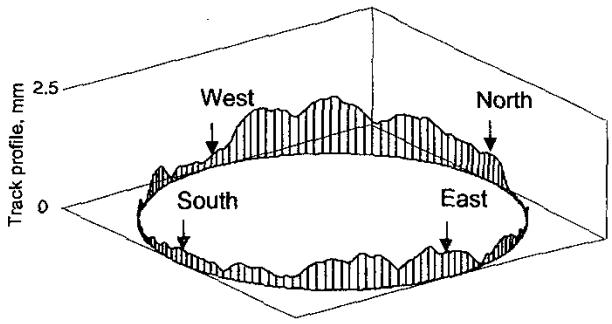


**Figure 1. The track profile of the DSS26 antenna.**

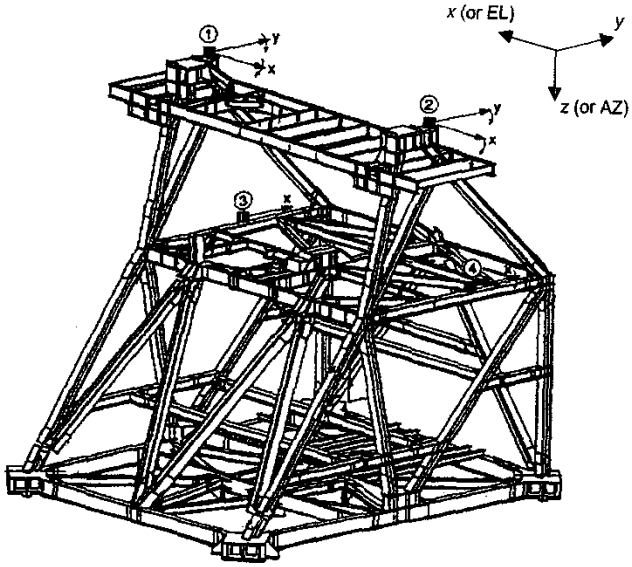


**Figure 2. The locations of the inclinometers on the alidade structure.**

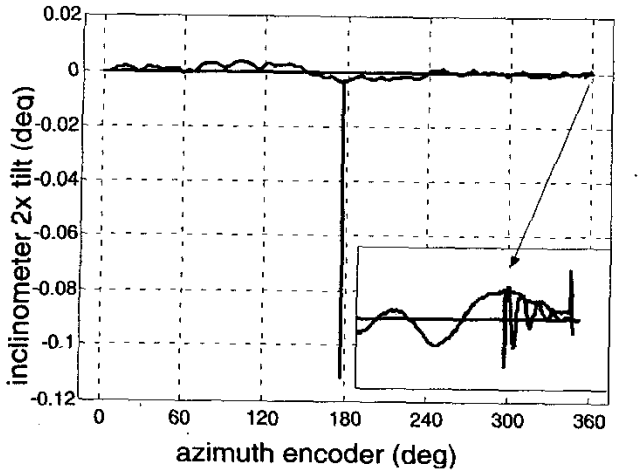


**Figure 3a. The data before Step 1 of the processing.**

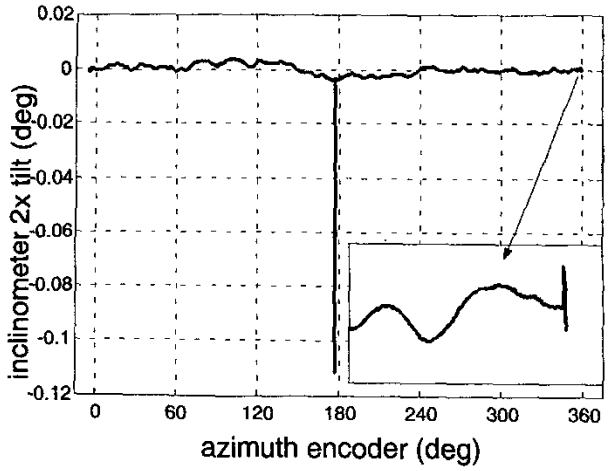


**Figure 3b. The data after Step 1. The overlapped part at 360° was moved to the beginning (at negative encoder values).**

encoder and inclinometer data are collected, and four sets are advised. Using the collected data, a lookup table is generated. The lookup table is computed at one-tenth-degree intervals, or azimuth angles from 0° to 360°. Additionally, the distances $h$ (the height from the azimuth track to Inclinometer 1) and $l$ (the distance between Inclinometers 1 and 2), in consistent units, are required for lookup-table creation.

The inclinometer data are noisy, contain occasional spikes, and include slowly varying trends. The noise must be filtered out and the spikes removed. The data-collection process lasts more than one hour, long enough for the antenna structure to be affected by the environmental temperature changes. These changes are visible in the inclinometer data as slowly varying trends (see [1]). The slow trends are identified in the Fourier transforms of the data as the low-frequency components. These components are subtracted from the data, with no evidence of trends in the new data. The low-frequency components also include the amplitude and phase of the antenna vertical-axis tilt.

## 3. Data Processing

The data processing consists of five steps:

1. Process the raw data
2. Filter
3. Move the negative segment
4. Perform a Fourier transform
5. Match the tilt at 0° and 360°.

The first step involves the reversal of the encoder and inclinometer data so that the encoder trend is clockwise, removing data whenever the antenna was stationary, and verifying that there is at least 365° of rotation. The $x$ tilts of the second inclinometer, $\alpha_{2x}$, before and after the first stage of processing, are shown in Figure 3 as examples, illustrating the above procedure.

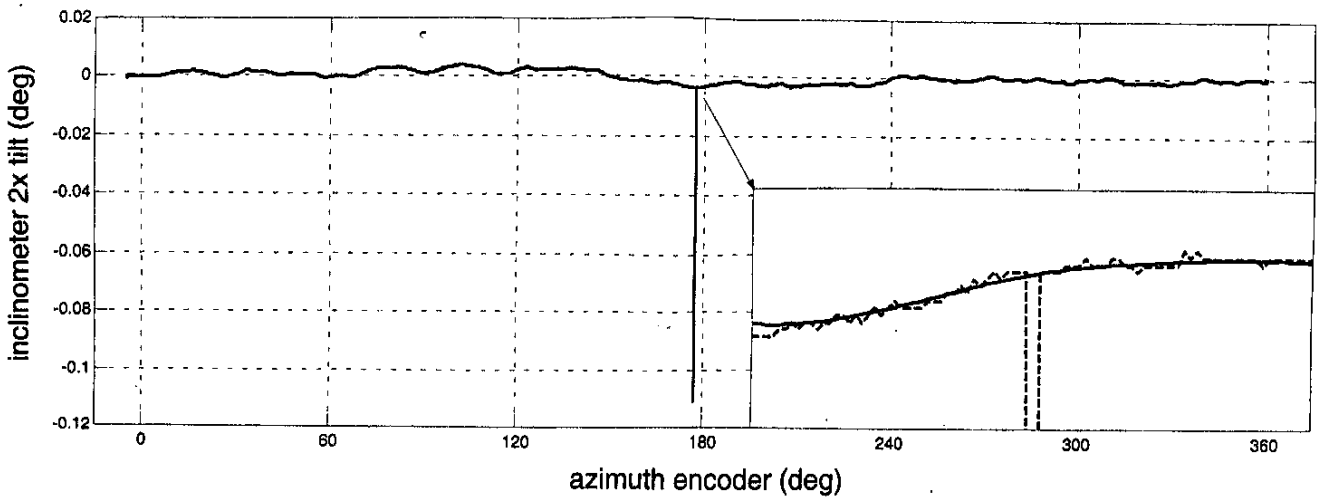


**Figure 4. The data before (dashed line) and after (solid line) Step 2 of the processing. The spikes have been removed, and the data have been smoothed.**

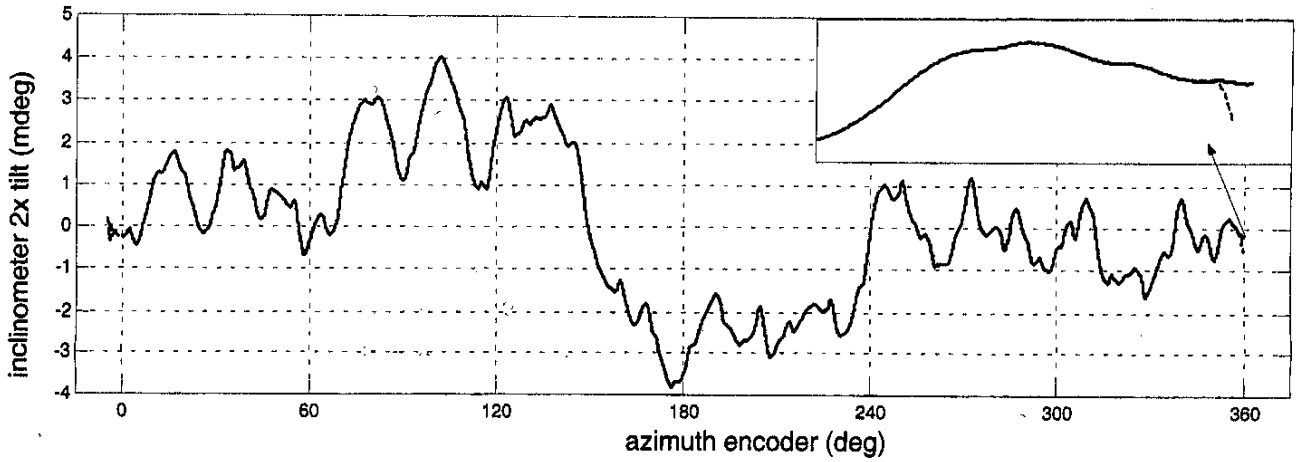


**Figure 5. The data before (dashed line) and after (solid line) Step 3 of the processing. After Step 3, the data fit the azimuth-angle segment of [0°, 360°], and the data outside the segments are removed.**

The second step (filtering) begins with the removal of inclinometer spikes, followed by inclinometer-data smoothing, using a zero-phase forward and reverse digital filter (*MATLAB*® filter `filtfilt.m`). The result has zero phase distortion, and its magnitude is smoothed. Forty points are cropped from each end of the inclinometer and encoder data to minimize startup and ending transients. The tilts, $\alpha_{2x}$, before and after this stage are shown in Figure 4. The figure shows a smoothed curve without spikes, after filtering.

In the third step, the negative segment of the data is shifted to the end. The negative segment of the data provides an overlapped segment that allows for the correct adjustment of the beginning and the end of the [0°, 360°] segment, and allows for verification of repeatability. The tilts, $\alpha_{2x}$, before and after this stage are shown in Figure 5. The figure shows the processed data that fit the azimuth-angle segment of [0°, 360°].

In the fourth step, the time-dependent thermal effects are removed by zeroing out the fundamental, second-harmonic, and third-harmonic terms of the transformed data, using *MATLAB*'s fast Fourier transform algorithm. The removal does not impact the antenna pointing, since the removed harmonics are the part of the pointing model that consists of a fourth-order spherical-harmonic expansion.

The three harmonics that were removed from the inclinometer data are shown in top three plots of Figure 6, and their sum is shown in the bottom plot of Figure 6 by the dashed line. In the latter figure, the inclinometer data are shown by solid lines. The superposition shows that the low-rate trend indeed was recovered. The data $\alpha_{2x}$ before and after this stage are shown in Figure 7. The figure shows that the low-frequency trends were removed.

The data may also contain encoder spikes. Encoder spikes in the data are created by software imperfections, and the spiked values are replaced with the average of the neighboring values. In this step, the spikes are removed, and the processed inclinometer data are interpolated for a 0°-360° range, sampled every 0.1°.

The final step of the data processing is to put the data in a standard format for easy comparison with other data sets. The lin-

ear trend is removed, so that 0° and 360° both have zero tilt. Also, the constant offset is removed, since it is included in the pointing model. The linear trend is an artifact, caused by a slow thermal drift present during the measurements.

## 4. Lookup-Table Creation

The lookup table consists of three rotations of the top of the alidade, denoted $\delta_x$, $\delta_y$, and $\delta_z$. The rotation $\delta_x$ is in the direction of the elevation angle, and is positive in the upward direction. The rotation $\delta_z$ is in the direction of the azimuth angle, and is positive in the clockwise direction. The rotation $\delta_y$ is orthogonal to the $\delta_x$ and $\delta_z$ angles, and is sensed so as to define a right-handed coordinate system. The coordinate system for these rotations is shown in Figure 2.

The three-axis lookup table is created using the $x$-axis tilts ($\alpha_{1x}$, $\alpha_{2x}$, $\alpha_{3x}$, and $\alpha_{4x}$) at four locations on the antenna structure, as well as the $y$-axis tilt of the inclinometer at the elevation encoder ($\alpha_{2y}$) (see Figure 2 for the locations and reference axes). Note that the downward inclinometer tilts are positive, and that the

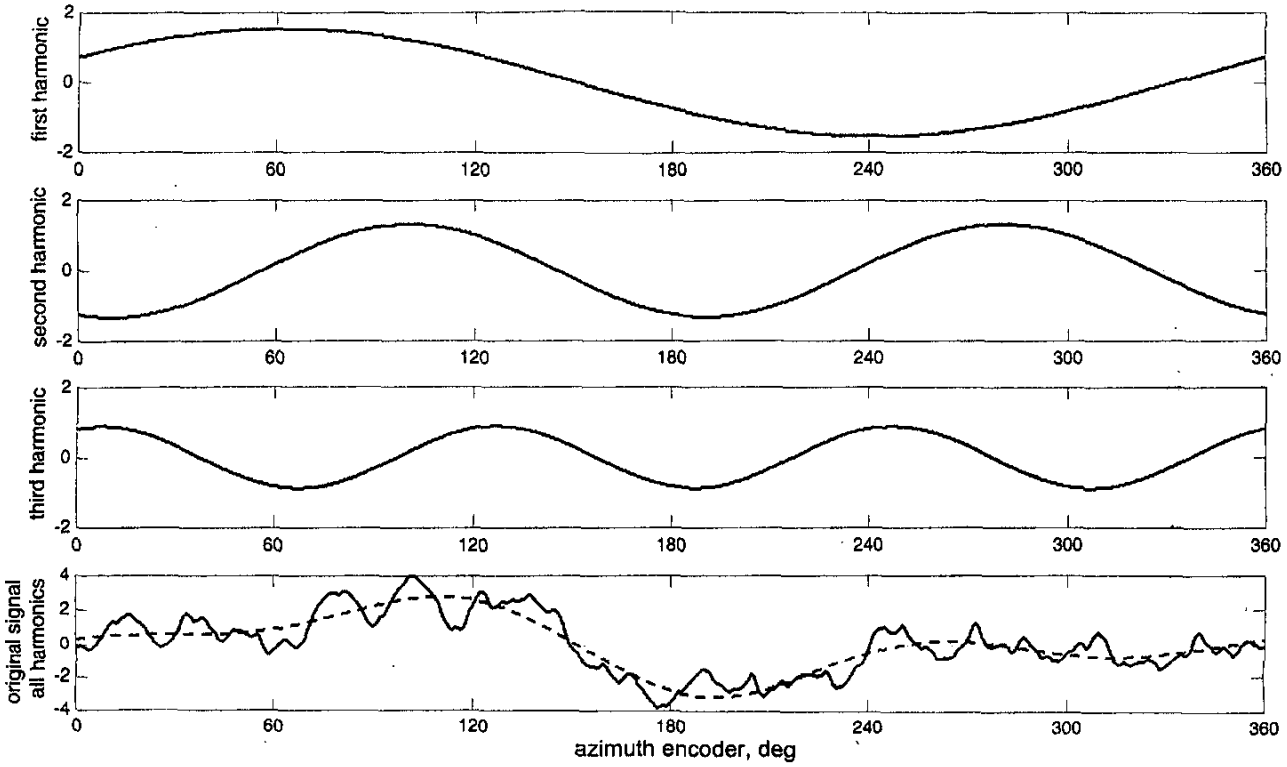


**Figure 6. The removal of trends. The top three plots show the first three harmonics of the inclinometer data in Figure 5. The bottom plot shows the sum of the first three harmonics (dashed line), on top of the inclinometer data (solid line).**

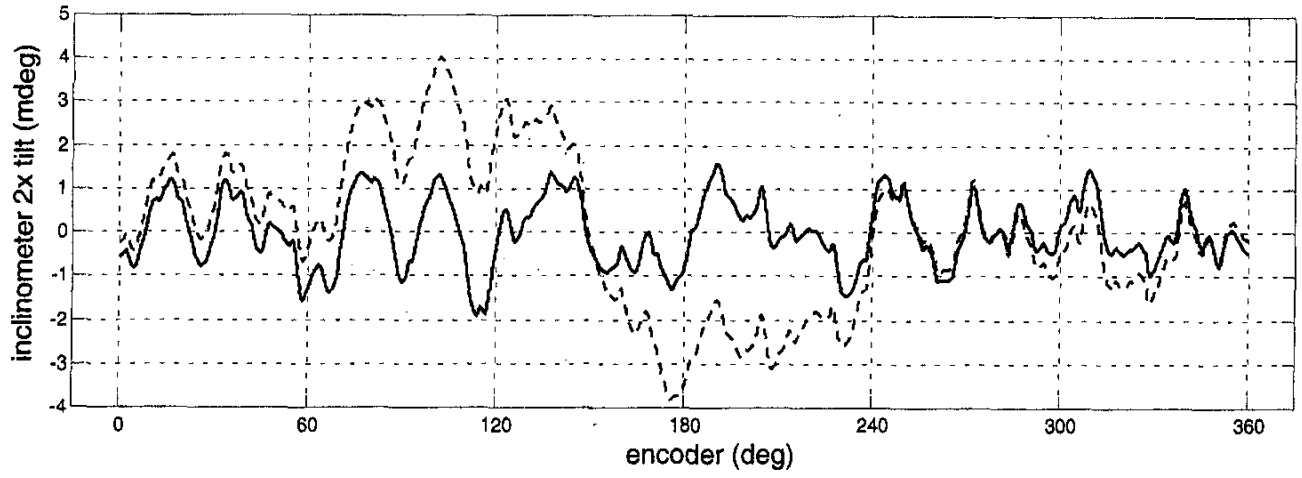


**Figure 7. The data before (dashed line) and after (solid line) Step 4: after this step, the slow trends have been removed.**

$x$ tilts of inclinometers 3 and 4 are parallel to the $y$ tilts of inclinometers 1 and 2. The alidade rotations are obtained in the following manner (see [1]):

$$\delta_x = \alpha_{2y}, \tag{1a}$$

$$\delta_y = -0.5(\alpha_{1x} + \alpha_{2x}), \tag{1b}$$

$$\delta_z = \frac{h}{l}(\alpha_{3x} - \alpha_{4x}). \tag{1c}$$

The lookup table is plotted in Figure 8.

For the given antenna elevation position ($\theta_{el}$), the azimuth, cross-elevation, and elevation pointing-error corrections are obtained from the lookup table components as

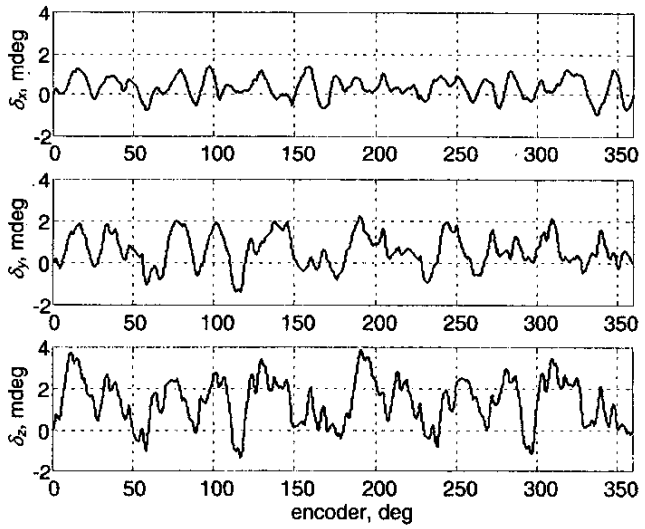


**Figure 8. The lookup table obtained from the processed data using Equations (1a-c). These are the alidade rotations $\delta_x$, $\delta_y$, and $\delta_z$ as a function of the azimuth-encoder angle.**

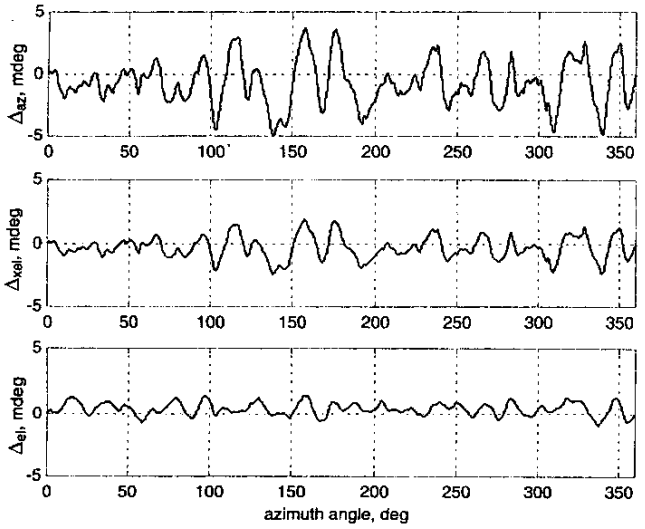


**Figure 9. The pointing-error corrections $\Delta_{az}$, $\Delta_{xel}$, and $\Delta_{el}$, obtained from the lookup-table values $\delta_x$, $\delta_y$, and $\delta_z$, using Equations (2a-c).**

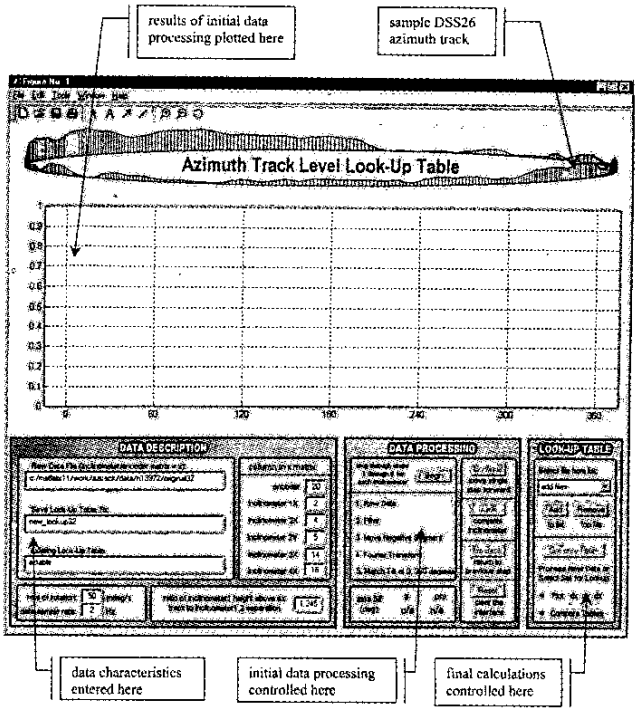


**Figure 10. The layout of the graphical user interface (GUI).**

$$\Delta_{el} = \delta_x, \tag{2a}$$

$$\Delta_{xel} = \delta_z \cos(\theta_{el}) - \delta_y \sin(\theta_{el}), \tag{2b}$$

$$\Delta_{az} = \delta_z - \delta_y \tan(\theta_{el}); \tag{2c}$$

see [1]. The pointing-error corrections for the elevation angle $\theta_{el} = 60°$ are plotted in Figure 9.

## 5. GUI Description

The presented graphical user interface (GUI) creates the lookup table, and uses raw measurement data, without initial processing. This interface contains three sections (see Figure 10): data description, data processing, and lookup-table generation, all of which are in the bottom half of the window. Additionally, three visual sections contain a plot in the interface, where the data are plotted during the processing phase; and external plots A and B, which display processed inclinometer tilts and the lookup table, respectively.

The data are entered into the GUI using the following steps (see the Data Description section of the GUI in Figure 10):

- Enter the data set into the "raw data file" editable text box
- Enter a new filename into the "save lookup table to" box
- Enter the distance ratio ($h/l$), using consistent units
- Verify that the columns of data are correctly indexed

The GUI displays the effects of data processing, such as smoothing, spike removal, trend removal using Fourier transform, aligning the data from 0° to 360°, and interpolating the data to a standard form.

The following steps process the data (see the Data Processing section of the GUI in Figure 10):

- Hit the "begin" button.
- Step through the computations using the "continue" button. Compute steps 1-5 for the following inclinometer tilts: $\alpha_{1x}$, $\alpha_{2x}$, $\alpha_{2y}$, $\alpha_{3x}$, and $\alpha_{4x}$. For each plot, a solid blue line represents the data just calculated, and a dotted green line represents the previous step.
- The "back" button takes a single step backwards to return to the previous step, if at any time the user chooses to view the results of one or more previous steps.
- The data processed thus far are saved in the file `guirun.mat`. The inclinometer values are stored under the lookup table pull-down list, and the individual inclinometer results are plotted in an external window, called Figure A. It is from this list that the user selects a file for lookup-table generation.

At least three complete inclinometer data sets should be processed to verify the repeatability of the data. A lookup table of $\delta_x$, $\delta_y$, and $\delta_z$ is generated from the representative data set. The user may verify the similarities between the newly processed and the existing lookup tables.

As data sets are processed, the results from each inclinometer are added to a subplot of an external Figure A, and the file is added to the pull-down menu. After processing a few sets, this figure should provide the information needed to compare the different sets, and the user can select one set with which to create a lookup table. This program then plots $\delta_x$, $\delta_y$, and $\delta_z$, the three lookup-table components, in another figure, called Figure B. These plots are shown in Figure 8. As an optional last step, the user may choose to add an existing lookup table to these plots for comparison. The pointing-error corrections are computed from Equations (2a-c), and plotted in Figure 9.

The following steps are required to obtain a lookup table (see the Lookup Table section of the GUI in Figure 10):

- The user must select one representative data set, rejecting those with the largest deviations from the others. To choose this set, that file is selected from the pull-down list. If desired, the user may remove the "bad" files from the pull-down list with the "remove" button.
- Press the "compute table" button. The variables $\delta_x$, $\delta_y$, and $\delta_z$ will be saved to the file entered in the "save file to" box, and the plot will appear in Figure B.
- If the Figure A window has remained open throughout all data processing, each file plotted should appear in the pull-down list.

## 6. Conclusions

This paper has described the processing of the field data (inclinometer tilts and azimuth-encoder reading) and the creation of the azimuth-track-level lookup table. It also explained the generation of the pointing-error corrections. The data processing and the creation of the lookup table are accomplished through a graphical interface that allows a user – not necessarily familiar with its creation procedures – to proceed to the end results, step-by step.

## 7. Acknowledgments

The authors thank Paul Richter of JPL for his discussions on the low-order trend calculations. The research described in this paper was carried out at the Jet Propulsion Laboratory, California Institute of Technology, under a contract with the National Aeronautics and Space Administration.

## 8. Reference

1. W. Gawronski, F. Baher, and O. Quintero, "Azimuth-Track-Level Compensation to Reduce Blind-Pointing Errors of the Deep-Space Network Antennas," *IEEE Antennas and Propagation Magazine*, **42**, 2, April 2000, pp. 28-38.

## Introducing the Feature Article Authors

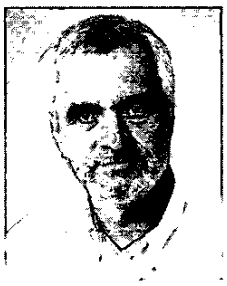

**Wodek Gawronski** received his MSc and PhD in mechanical engineering from the Technical University of Gdansk, Poland. He was a professor of dynamics and controls at the Technical University of Gdansk and at the University of Hanover, Germany. Later, he was a NRC Senior Fellow at the NASA Langley Research Center, Hampton, Virginia, working on spacecraft structural dynamics and control problems. Currently, he is Engineering Principal in the Communication Ground Systems Section, Jet Propulsion Laboratory, responsible for the control-system analysis and design of the NASA Deep Space Network antennas. He was also a consultant on control-system design to several radio telescope projects, including the NRAO 100-meter Green Bank Telescope, West Virginia, and the 50-meter Large Millimeter Wavelength Telescope in Pueblo, Mexico.

**Erin Maneri** received her Bachelor of Science degree in Applied Mathematics at Montana State University in 2000. During her cooperative tour at the Jet Propulsion Laboratory, California Institute of Technology, she worked on antenna pointing and tracking tasks. She is currently attending graduate school at the Massachusetts Institute of Technology. She has also engaged in independent research projects funded by Women in Science and Engineering and the National Science Foundation. Erin's other technical interests include mathematical modeling and medical applications of control systems.

**Editor's Comments** *Continued from page 8*

ses. They state in their article that part of its purpose is to initiate a dialog on these subjects. As always, the pages of this *Magazine* are open for such a dialog. I found this to be a very thought-provoking discussion, and one that helped to significantly clarify concepts that are often masked by the mathematics and/or specialized terminology of other presentations. I think you will, too.

## Our Other Contributions

Be sure to read Wilson Pearson's contribution to Cynthia Furse's Education Column. It has a very imposing title – involving "operational calculus," no less – but what is really involved is simple, straightforward, elegant, and easily understood. It involves the use of two-dimensional Fourier transforms to relate the field in the aperture of an array to the field radiated by the array. Various properties of the Fourier transform permit simple expressions for the effects of the regular spacing of the array elements, and make it easy to derive the convolution relationship for the array pattern in terms of the array factor. Fourier-transform properties also make it easy to derive the effects of array-element spacing on grating lobes. If you're not familiar with this approach, you should be.

In Tom Milligan's Antenna Designer's Notebook, Francisco Ares and his colleagues from the Universities of Santiago de Compostela and Coruña describe how to design the excitation of a planar array using a neural network. The application used to demonstrate this is the shaping of the beam of a communications-satellite antenna, although the technique could be applied in many other situations, as explained in the contribution. It is a very nice result, and has the advantage of being quite efficient, computationally. Readers should note that a companion feature article will appear in the next issue of the *Magazine*. I apologize that our page budget is such that we couldn't include it in this issue (Fortunately, the AdCom has already approved an increased page budget for next year: keep those contributions coming!)

In Christos Christodoulou's and Tuli Herscovici's Wireless Corner, Salvatore Bellofiore, Jeffrey Foutz, Constantine Balanis, and Andreas S. Spanias present the second part of their two-part review of smart-antenna systems. In this issue, they look at the signal processing involved. Specifically, they consider how direction-of-arrival algorithms are used to tailor the radiation pattern of the antenna. Examples simulating a continuously changing network are given.

Peter Staecker, our Division IV Director, has provided us with another update on the financial situation of the IEEE. Progress is being made, which is good. Peter has done an outstanding job of representing our Society's interests on the IEEE Board of Directors. Equally important, he has done an outstanding job of communicating what is actually going on at the Board level, and with the finances of the IEEE, to those he represents. He will finish his term at the end of this year. He deserves our thanks. Hal Flescher, who has been serving as TAB Treasurer, will be our new Division IV Director. I extend to him the same invitation to which Peter so admirably responded: please use the pages of our *Magazine* to keep us up-to-date on any and all issues of interest to our members.

I have had the pleasure of working with Bob Hunsucker, in both AP-S and URSI, for many years. Bob has most recently done an outstanding job of being Editor-in-Chief of the journal *Radio Science* for the last eight years. Bob is also a Ham. In this issue, he shares some of his memories of how he became a Ham, and of the influence this has had on his career as a radio scientist.

## Image Quality in the *Magazine*

I commented in my column in the April issue about problems we have had with the quality of photographs and some line art in the *Magazine*. While the April issue was relatively free of these problems, they occurred again in the June issue. These have been intermittent, and it has therefore been difficult to identify the cause. I've recently had a number of discussions about the problems with Bob Smrek, the IEEE Director of Periodicals Production and our interface to the printer, and with the staff of the printer (and I really appreciate the efforts of Bob and our printer in trying to help solve the problems). It turns out that there are probably several factors involved. As I noted in April, a major factor is that at some point last year, the printer changed from using a photographic process to produce the printing plates to using a digital process. This change implied changes in the effective resolution and tonal range of the digitally produced "halftones" made from photos, as compared to what was being done with a photographic screening process. We've also discovered that a variety of effective line-screen values were being used, instead of employing a screen value optimized for the types of photographs, the printing process, and the paper we use. Hopefully, the printer will be successful in eliminating these variations.

It also appears that we may need to change the paper we have been using: contrary to what I had previously understood, we may be able to improve the result by using a smoother paper with a different coating. It is possible you may even see an experiment with that in this issue. However, we will try to avoid going to the type of high-reflectance, "shiny" papers that are used by some magazines. A very shiny paper simply increases eyestrain for the reader.

## Free Advertising!

In his President's Message, Magdy Iskander has called for more participation in AP-S by our members from industry. As one

*Continued on page 39*